THE UNSTEADY LIQUID FILM FLOW OF THE CNTS-ENGINE OIL NANOFLUID OVER A NONLINEAR RADIALLY EXTENDING SURFACE

Abdullah K. ALZAHRANI[a], Malik Z. Ullah[a], Taza GUL[b] , Dumitru BALEANU[3, 4]

[a]Department of Mathematics, King Abdul Aziz University, Jeddah 21577, Saudi Arabia,

[b]Department of Mathematics, City University of Science and Information Technology, Peshawar,Pakistan.

[c]Department of Mathematics, Faculty of Arts and Sciences, Cankaya University, 06530 Ankara, Turkey.

[d]Institute of Space Sciences, P. O. Box, MG-23, R 76900, Magurele-Bucharest, Romania.

*Corresponding author: Email dumitru@cankaya.edu.tr

The enhancement of heat transfer through carbon material is the objective of this study. The renowned class of carbon identified as SWCNTs (single walled carbon nanotubes) and MWCNTs (multi walled carbon nanotubes) nanofluid flow over a nonlinear and unstable surface has been explored. The thermophysical properties of the two sorts of CNTs have been implemented from the experimental outputs in the existent literature using engine oil as a base fluid. The viscous dissipation term has also been included in the energy equation to improve the heat transfer rate. The thickness of the nanofluid thin layer is kept variable under the influence of the unstable and nonlinear stretching of the disk. The elementary governing equations have been transformed into coupled nonlinear differential equations. The problem solution is achieved through BVP 2.0 package of the OHAM (Optimal Homotopy Analysis Method). The square residual error for the momentum and thermal boundary layers up to the 20^{th} order approximations have been obtained. The numerical ND-Solve method has been used to validate the OHAM results. The impact of the model parameters versus velocity field and temperature distribution have been shown through graphs and tables. The impact of the physical parameters on the temperature profile and velocity, pitch for both MWCNTs and SWCNTs is gained in the range of $0 \le \phi \le 4\%$. From the obtained results it is observed that the SWCNTs nanofluids are more efficient to improve the heat transfer phenomena as compared to the MWCNTs.

Keywords: Carbon nanotubes-Engine oil based nanofluid, nonlinear flexible and unstable disc, Magnetic Field, Viscouse dissipation, Drag force and Heat Transfer rate, OHAM-BVPh 2.0.

1. Introduction

The Carbon nanotube (CNT) is the most important class of Carbon family, which have exceptional thermal, chemical, mechanical, electronic and optical properties. The astonishing properties of the CNTs have positioned them quite important for the mechanical engineering and materials sciences. Endo and Co-workers [1] were the pioneers to describe the TEM images of the CNT. Iijima [2] have investigated the tube- like nanosized CNTs in diameter range 4-30nm. The idea of single wall carbon nanotubes (SWCNTs) was established by two research groups [3,4].

Later on, this idea was more explained by To [5] to specify that the bending of graphene sheet in small nanosized known as CNTs. This study also categorized CNTs in its two core classes named

single and multi wall carbon nanotubes and abbreviated as (SWCNTs) and (MWCNTs). The size of the SWCNT is 1nm while MWCNTs is in the form of a cluster containing 2-50 concentric tubes with 0.34nm spacing.

The imperative applications of CNTs are mostly related to energy alteration, electronics and automotive. CNTs are in the metal shape and can improve electricity and heat transfer rate [6,7]. The use of the CNTs in the field of mechanical engineering EOR for the oil recovery was utilized by Negin et al. [8]. Nieto de Castro and Murshed [9] have studied the thermal properties of a special type of nanofluids called ionofluids. Inonofluids contain some exceptional property and due to this property concentration and temperature carbon nanotube increased. Zaidi et al. [10] Inspected nanofluid of carbon nanotube flow of wall jet streaming by means of the convective physical state using a numerical method.

The stable dispersion of CNTs in various liquids accomplishes the CNTs nanofluids. The useful base liquids which are suitable for the synthesis of CNTs are water, Ethylene glycol and engine oils. Various of the researchers [11-19] have utilized the above-mentioned base fluids for the stable dispersion of CNTs.

The diversities of models exhibit in the literature to describe the thermal conductivities of carbon nanotubes in the varieties of structures. The efforts done by the researchers to define a comparative model for the improvement of the thermal conductivities of CNTs are Maxwell [20] , Jeffery [21], Davis model [22], Lu and Lin [23] and Crosser [24]. All the above researchers have done the significant work for the enhancement of heat exchange by introducing the thermal conductivity models and these models are used for the various nano materials.

Xue [25] suggested a model of the for the suitable dispersion of CNTs depending on the shape and properties of CNTs.

In the past much attention has been paid to the steady flows over the linearly stretchable surfaces. Still a lot of work is required to be reported for the fluid flow over an unsteady and nonlinear stretched surfaces [26-29].

The liquid film diffusion has substantial applications in the arena of science and manufacturing. The uses of coating in different industries like fiber coating used for telecommunication purposes, coating of the sheets cylinder disc [30] etc. Shah et al. [31] have studied the this film flow of nanofluid over a linearly stretching and rotating disk [31]. Recently, Gul [32] have examined the liquid film sprinkling over a nonlinear enlarging surface. Ghanj [33], have studied the liquid film flow of non-Newtonian fluids using the oscillatry geometry. Gohar et al. [34] have reflected the steady flow of the CNTs over a nonlinear enlarging disc. They studied the single and multi walled carbon nanotubes considering the steady flow of the water based nanofluid. Qasim et al. [35] conferred the unsteady flow of the thin nanoliquid layer using Buongiorno's model. The thin film spray of the nanofluid over an extending tube for the thermal and cooling applications has been studied by Wang [36] and Khan et al. [37]. Alshomrani and Gul [38] have extended the spray of a nano liquid film over the slippery surface of an extending cylinder.

Keeping in mind the above meaningful work the purpose of the recent work to analyze the liquid film flow of a SWCNTs/MWCNTs-Engine oil based nanofluid flow over an unstable and nonlinearly extending surface. The solution of the transformed nonlinear equations is achieved by a well-known analytical technique OHAM (Optimal Homotopy Analysis Method) [39,40]. Advance version of this technique (BVP-2) has been used for the error analysis which authenticates the

convergence of the obtained results. The Mathematica Package BVPh 2.0 for Nonlinear Boundary Value Problems has been adopted by Zhao et al. [41], and this package is frequently used for the high nonlinear problems [42-44] in various engineering problems. Furthermore, the validation of this method has been checked by the researchers [45,46] with the existing literature. The influence of the modeled different parameters under the influence of SWCNTs/ MWCNTs is calculated successfully.

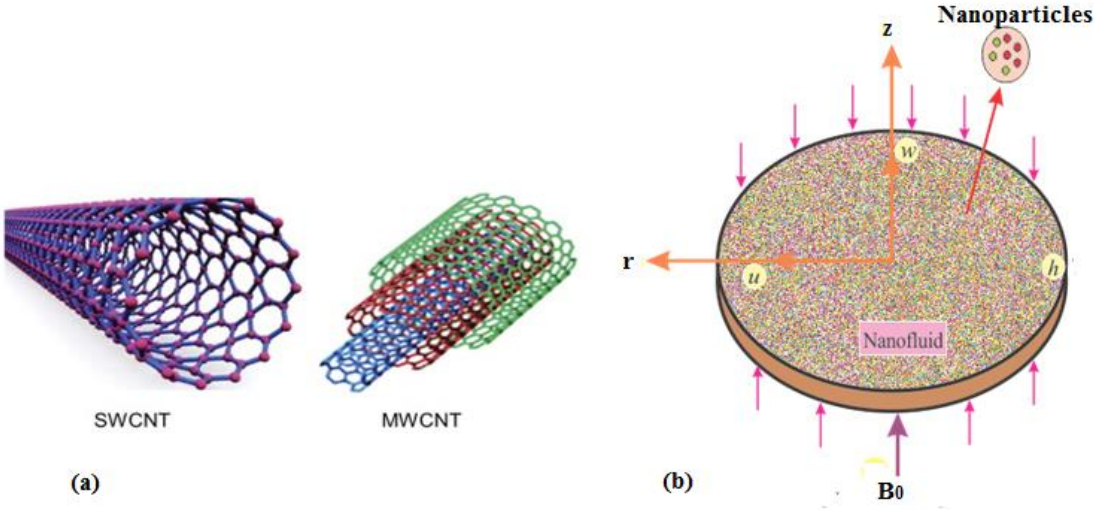

Figure. 1: (a) SWCNTs and MWCNTs **(b)** Physical interpretation of the problem.

1.1. Problem Formulation

A thin film of SWCNTs/MWCNTs engine oil based nanofluids is considered over an unsteady and nonlinearly extending disc. Initially the disc is positioned at $z=0$ and $z=h$ is limited thickness of thin film nanofluid. The nonlinear velocity $U_w=\frac{ar^n}{(1-bt)}$ is used for the stretching of the disc. Where $n=1$ represent the linear stretching and $n=2,3,4...$ represent the extending nonlinear disc. The radius of the disc is presented by r and t is the time. The magnetic field acts perpendicularly to the fluid flow direction. Let us suppose that the pressure is atmospheric, on behalf of this pressure term is vanished. The continuity, momentum and energy equations for the unsteady nanofluid flow are identified as:

$$\frac{\partial u}{\partial r}+\frac{u}{r}+\frac{\partial w}{\partial z}=0, \tag{1}$$

$$\rho_{nf}\left(\frac{\partial u}{\partial t}+u\frac{\partial u}{\partial r}+w\frac{\partial u}{\partial z}\right)=\left(\mu_{nf}\frac{\partial^2 u}{\partial z^2}-\sigma_{nf}B_0^2 u\right), \tag{2}$$

$$(\rho Cp)_{nf}\left(\frac{\partial T}{\partial t}+u\frac{\partial T}{\partial r}+w\frac{\partial T}{\partial z}\right)=\left(k_{nf}\frac{\partial^2 T}{\partial z^2}+\mu_{nf}\left(\frac{\partial u}{\partial z}\right)^2\right). \tag{3}$$

The initial and boundary conditions prepared for our model is given below:

$$\begin{aligned} &u=U_w, w=0,\ \Theta=\Theta_w,\ \text{at z}=0,\\ &\mu\frac{\partial u}{\partial z}=\frac{\partial \Theta}{\partial z}=0, w=\frac{dh}{dt},\ \text{at z}=h. \end{aligned}, \tag{4}$$

The stream function $\psi(r,z) = -r^2 U_w \mathrm{Re}^{-\frac{1}{2}} f(\eta) \text{and} \eta = \frac{z}{r}\mathrm{Re}^{\frac{1}{2}},$ was used for the similarity transformation of the prevailing equations. The components of velocity are transformed as $u = -\frac{1}{r}\frac{\partial \psi(r,z)}{\partial z} = U_w f'$, and $w = \frac{1}{r}\frac{\partial \psi(r,z)}{\partial r} = -U_w \mathrm{Re}^{\frac{-1}{2}}\left[\left(\frac{3+n}{2}\right) f + \left(\frac{n-1}{2}\right)\eta \frac{df}{d\eta}\right]$ along the radial and axial direction respectively. Mathematically Reynold number in our model $\mathrm{Re} = \frac{rU_w}{\upsilon_f}$.

$T = T_0 - T_{ref}\left(\frac{U_w^2}{2a\upsilon_f}\right)\Theta(\eta)$ is used for the transformation of the energy equation in which T_{ref}, signifies reference temperature. After applying the transformation temperature and velocity components in the Eqs. (1-4) which satisfy the continuity equation and the rest of the equations have been attained as:

$$f''' + (1-\phi)^{2.5}\left((1-\phi) + \phi\frac{\rho_{CNT}}{\rho_f}\right)\left(\left(\frac{3+n}{2}\right) ff'' - n(f')^2 - S\left(f' + \frac{\eta}{2} f''\right)\right) - (1-\phi)^{2.5} Mf' = 0, \tag{5}$$

$$\frac{k_{nf}}{k_f}\Theta'' + \mathrm{Pr}(1-\phi)^{2.5}\left((1-\phi) + \phi\frac{(\rho c_p)_{CNT}}{(\rho c_p)_f}\right)\left[\left(\frac{3+n}{2}\right) f\Theta' - 2n(\Theta f')\right] + (1-\phi)^{-2.5} Ec\,\mathrm{Pr}(f')^2 = 0, \tag{6}$$

$$f(0) = 0,\ f'(0) = 1, \Theta(0) = 1,$$
$$f''(\beta) = 0,\ \left(\frac{n+3}{2}\right) f(\beta) + \left(\frac{n-1}{2}\right)\beta f'(\beta) = \frac{S\beta}{2},\ \Theta'(\beta) = 0. \tag{7}$$

The model suggested by Xue [25] has been used due to great axial ratio and repaying the CNTs space dispersal. The thermal conductivity of the CNTs nanofluids has been calculated using this model as: In equation (7) for linear stretching ($n = 1$) the conditions match to the published work [31].

The mathematical representation of the density of nanofluid is $\rho_{nf} = (1-\varphi)\rho_f + \varphi\rho_{CNT}$, where ρ_{CNT} indicates carbon nanotubes density and φ show nanoparticle volume fraction. Dynamic viscosity of nanofluid is in the form of $\mu_{nf} = \mu_f (1-\phi)^{\frac{10}{25}}$. Formula of kinematic viscosity used in our model can be written as $\upsilon_{nf} = \mu_{nf}(\rho_{nf})^{-1}$. The term $(\rho C_p)_{nf} = (1-\varphi)(\rho C_p)_f + \varphi(\rho C_p)_{CNT}$, denote the nanofluid capacity of specific heat specific heat. $\beta = r^{-1}h\,\mathrm{Re}^{\frac{1}{2}}$, is the thin film thickness of the nanofluid. $M = {r\sigma_{nf}B_0^2}\big/{(\rho_f U_w)} = {\sigma_f B_0^2(\rho_f a)}\big/{r^{(n-1)}}$ is the dimensionless magnetic field. The

Prandtl number is represented by $\Pr = {\mu_f Cp}/{k_f}$ and $Ec = {U_w^2}/{(C_p)_f \Delta T}$ is the Eckert number. The parameters used for engineering purposes are Nusselt number and skin fraction which can represent as $C_f = {2\tau_w}/{\rho_{nf} U_w^2}$ and $Nu = {r^n q_w}/{k_{nf} \nabla T}$ respectively.

The wall stress $\tau_\omega = \mu_{nf}\left(\frac{\partial u}{\partial z}\right)_{z=0}$ and heat flux $q_w = -k_{nf}\left(\frac{\partial T}{\partial z}\right)_{z=0}$ have been inserted to the discussed parameters as:

$$\frac{1}{2}\mathrm{Re}^{\frac{1}{2}}(1-\varphi)^{\frac{25}{20}}\sqrt{\left((1-\phi)+\phi\frac{\rho_{CNT}}{\rho_f}\right)}C_f = -f''(0),\quad \frac{\mathrm{Re}^{\frac{-1}{2}}(1-\varphi)^{\frac{20}{25}}}{\sqrt{\left((1-\phi)+\phi\frac{\rho_{CNT}}{\rho_f}\right)}}Nu = -\Theta'(0). \tag{8}$$

1.2. OHAM- BVPh 2.0 Package

The BVPh-2.0 package of OHAM [38-40] has been applied for the solution of the modeled equations (5,6) with the physical conditions in equation (7).

The 20th order approximation has been obtained and the residual error has been minimized for the stable convergence of the obtained results. The resulting linear operators and initial trials which have an important role in the OHAM solution are selected as:

$$f_0(\eta) = \frac{1}{(3+5n)}\left[(3+5n)\eta - (2+2n-5)\right]\left(\frac{3}{\beta}\eta^2 - \frac{1}{\beta^2}\eta^3\right),\ \Theta_0(\eta) = 1. \tag{9}$$

Suppose the linear operators λ_f and λ_Θ are defined as:

$$\lambda_f = \frac{\partial^4}{\partial\eta^4} \quad \text{and} \quad \lambda_\Theta = \frac{\partial^2}{\partial\eta^2}, \tag{10}$$

Thus the common result of λ_f and λ_Θ is

$$\lambda_f\left[\lambda_1 + \lambda_2\eta + \lambda_3\eta^2 + \lambda_4\eta^3\right] = 0 \quad \text{and} \quad \lambda_\Theta\left[\lambda_5 + \lambda_6\eta + \lambda_7\eta^2\right] = 0. \tag{11}$$

According to the essential information of OHAM clarified in [38 ,40], equations (5,6) are validated as

$$\varepsilon_m^f = \frac{1}{\lambda+1}\sum_{j=1}^{\lambda}\left[\aleph_f\left(\sum_{i=1}^{m} f(\eta)\right)_{\xi=j\delta\xi}\right]^2, \tag{12}$$

$$\varepsilon_m^\Theta = \frac{1}{\lambda+1}\sum_{j=1}^{\lambda}\left[\aleph_\Theta\left(\sum_{i=1}^{m} f(\eta), \sum_{i=1}^{m}\Theta(\eta)\right)_{\xi=j\delta\xi}\right]^2, \tag{13}$$

Liao [38,39] was the first that defined total squared residual error using OHAM

$$\varepsilon_m^t = \varepsilon_m^f + \varepsilon_m^\Theta. \tag{14}$$

The auxiliary parameters have been used and the total residual error ε_m^t has been obtained from the velocity field and temperature distribution respectively. The numerical values of the optimal convergence control parameters $h_f = -0.62701235, h_\Theta = -1.234102321$ have been archived in case of the SWCNTs while $h_f = -0.63120543, h_\Theta = -1.1356213021$ has been obtained in the case of MWCNTs. This method has the tendency to obtain the solution of the nonlinear differential equation without discretization in short time with residual error. Due to this fact, this method is frequently used in the recent research [38-45]. Furthermore, the increasing order of approximation reduces the square residual error which leads to the close convergence of the problem.

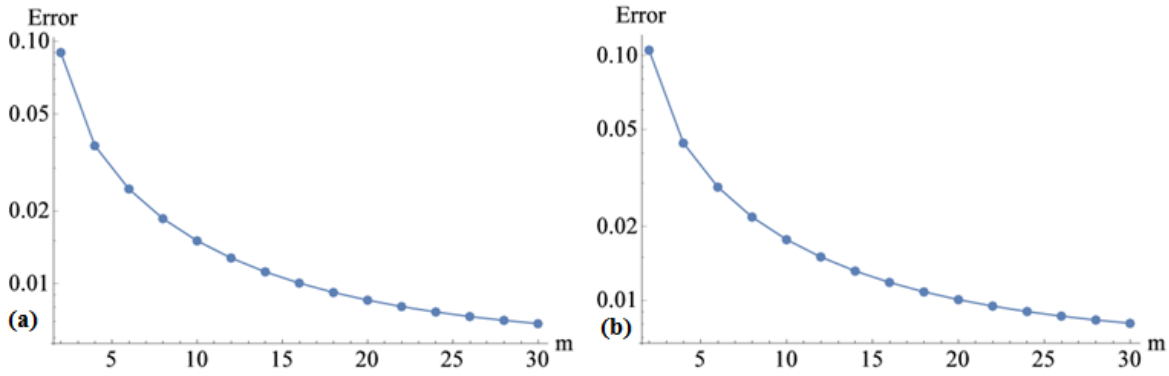

Figure. 2: Total Residual error OHAM up to 30th order approximation of **(a)** SWCNTs **(b)** MWCNTs.

The appropriate range of the physical parameters has also been calculated through OHAM and displayed. The obtained range of parameters for the proposed problem authenticates the convergence of the obtained results.

1.3. Results and Discussion

The thin film flow of CNTs nanofluid over an unstable and nonlinear radially stretching disc have been concentrated in this research. The SWCNTs/MWCNTs-engine oil based nanofluid has been utilized within the range $0 \le \phi \le 10\%$. The OHAM-BVPh-2.0 package has been used for the solution of the problem. Figure 1 (a) display the shapes of SWCNTs and MWCNTs while Figure 1 (b) shows the geometry of the problem. In Figure 2 (a) the square residual error for the momentum and thermal equations are reflected using the BVPh-2.0 package. The convergence for the 30th order of the OHAM method have been calculated and from the residual error, it is observed that the strong convergence has been started from the 20th iteration using the SWCNTs.The 30th order convergence using the MWCNTs has been obtained through the OHAM method and displayed in Figure 2 (b). It is observed that the residual error analysis authenticates the strong convergence of the OHAM method at the 10th iteration.

The suitable range of the physical parameters and their impact on the fluid motion have been illustrated in Figures. 3-15.

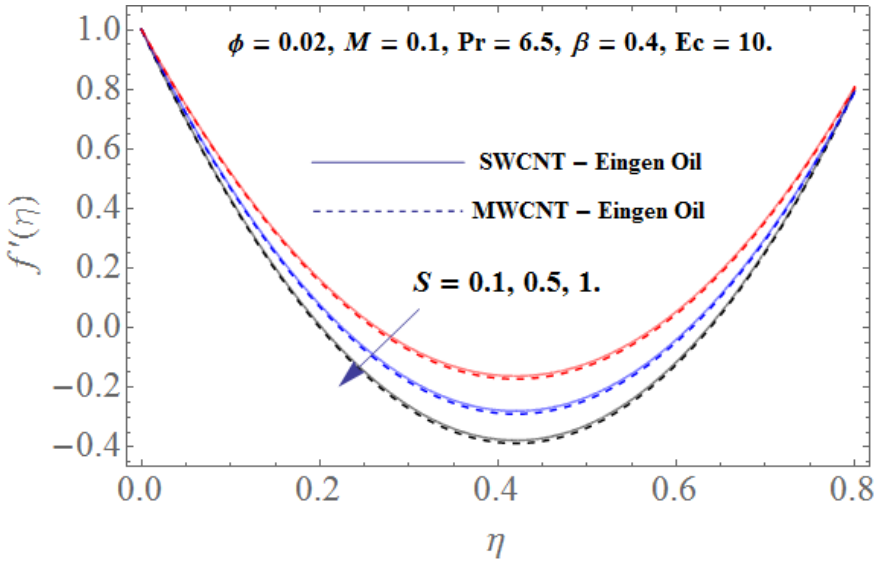

Figure. 3: The impact of the unsteady parameter S on the velocity field $f'(\eta)$.

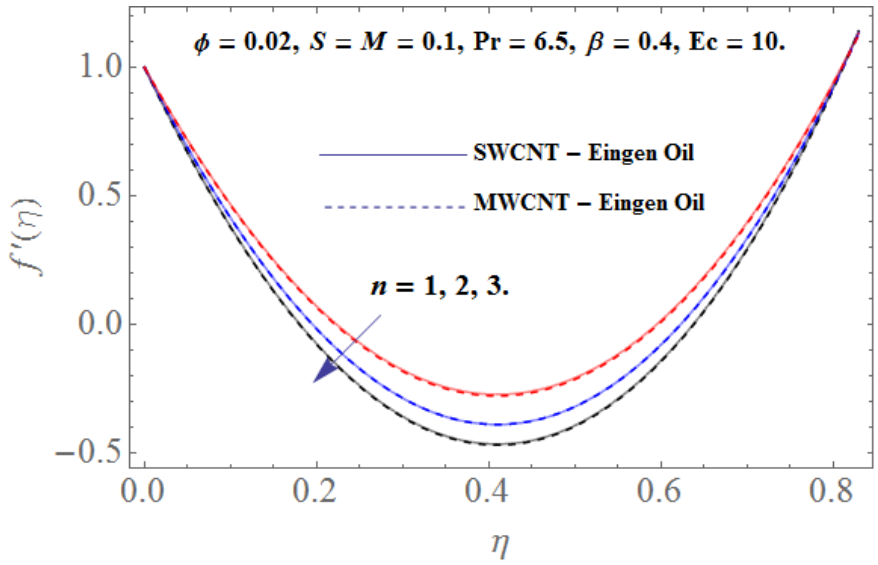

Figure. 4: The impact of the nonlinear stretching parameter n on the velocity field $f'(\eta)$.

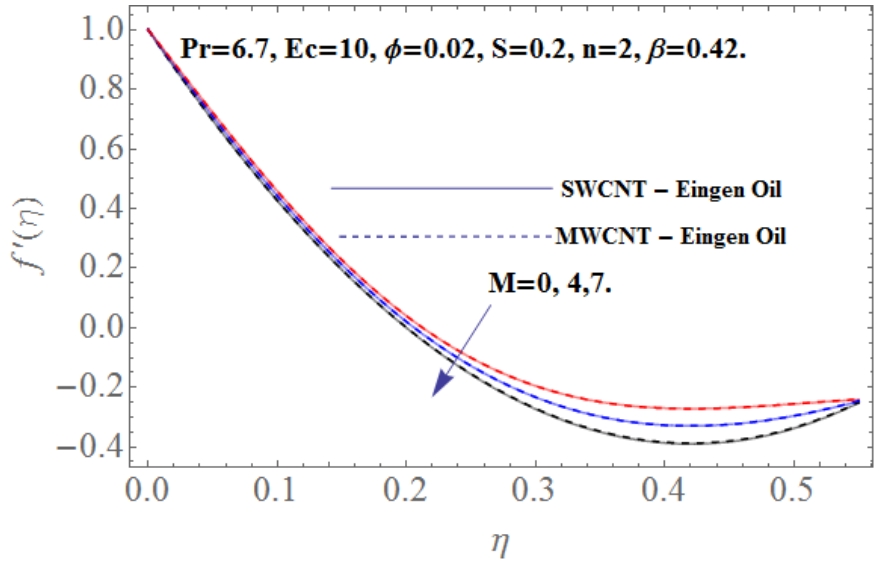

Figure. 5: The impact of the magnetic parameter M on the velocity field $f'(\eta)$.

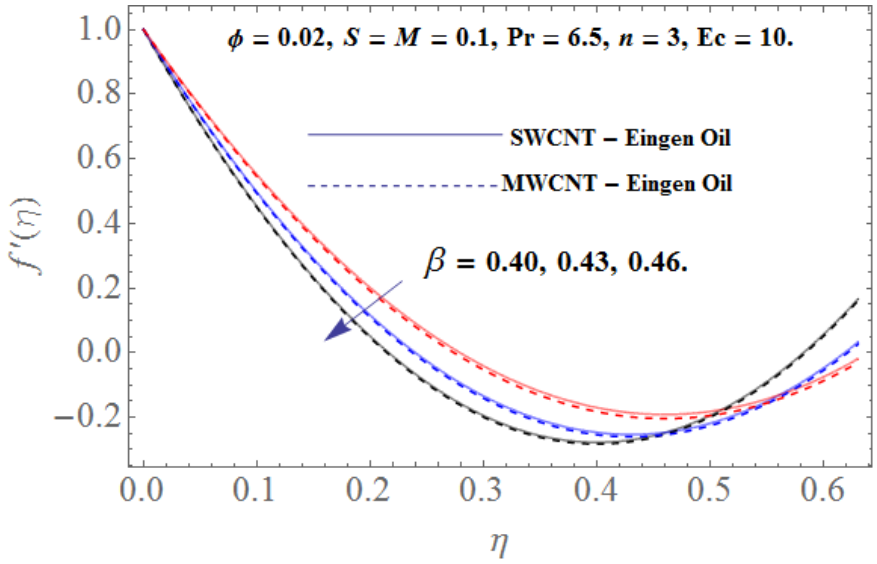

Figure. 6: Thickness parameter β versus $f'(\eta)$.

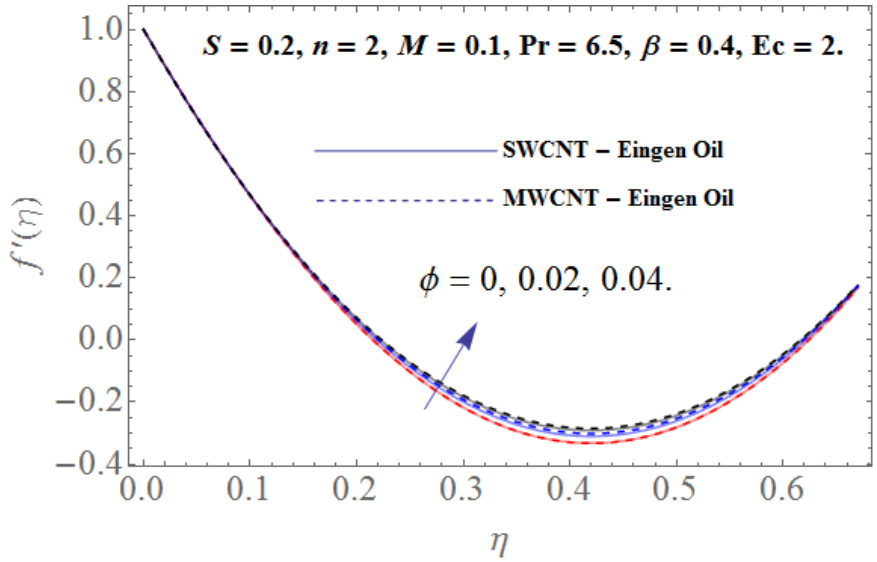

Figure. 7: ϕ versus velocity field $f'(\eta)$.

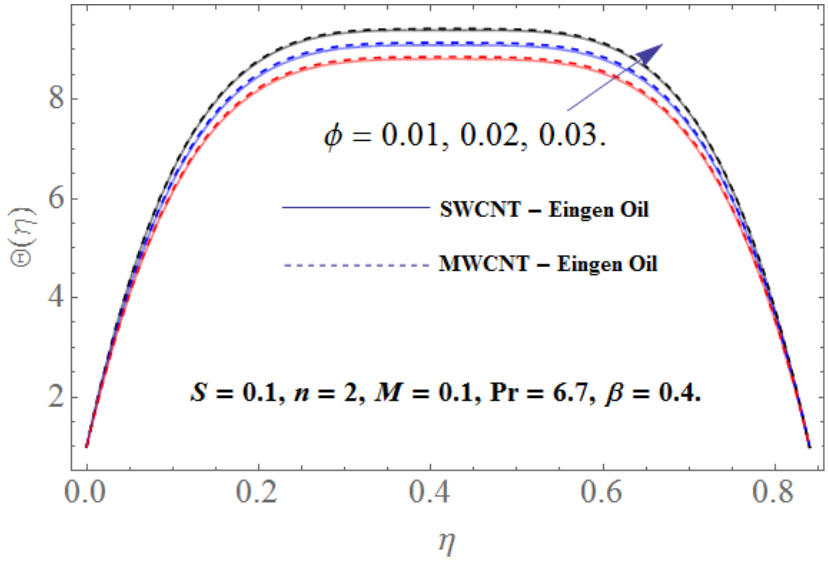

Figure.8: Nano particle volume fraction ϕ versus $\Theta(\eta)$.

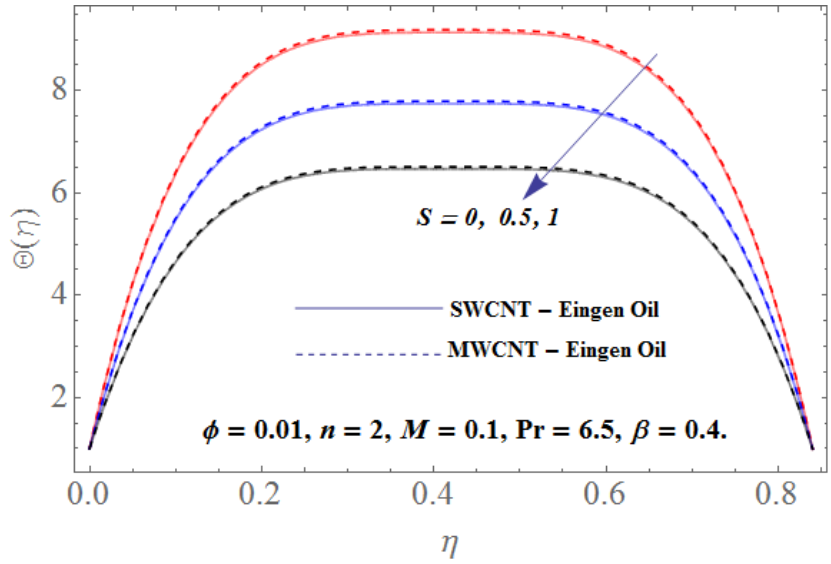

Figure.9: The impact of the unsteadiness parameter S on the temperature field $\Theta(\eta)$.

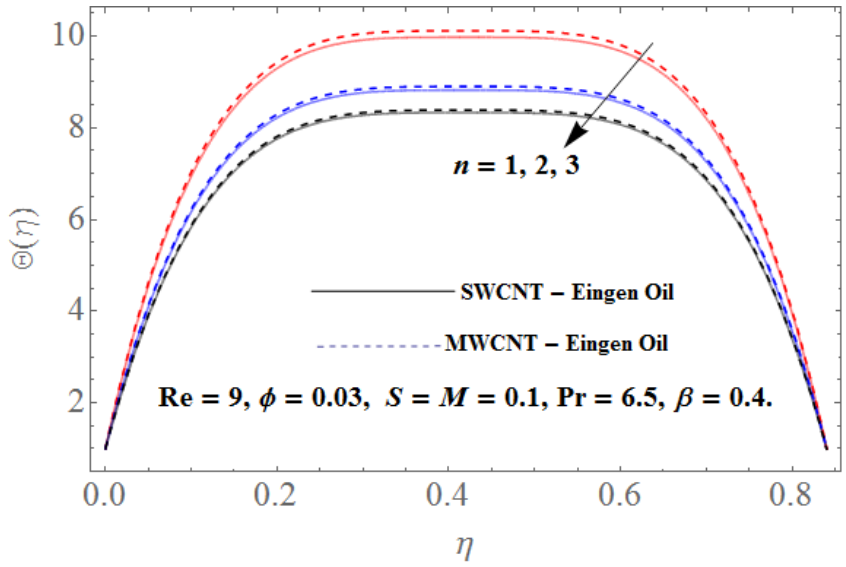

Figure. 10: The impact of the nonlinear stretching parameter n on the temperature field $\Theta(\eta)$.

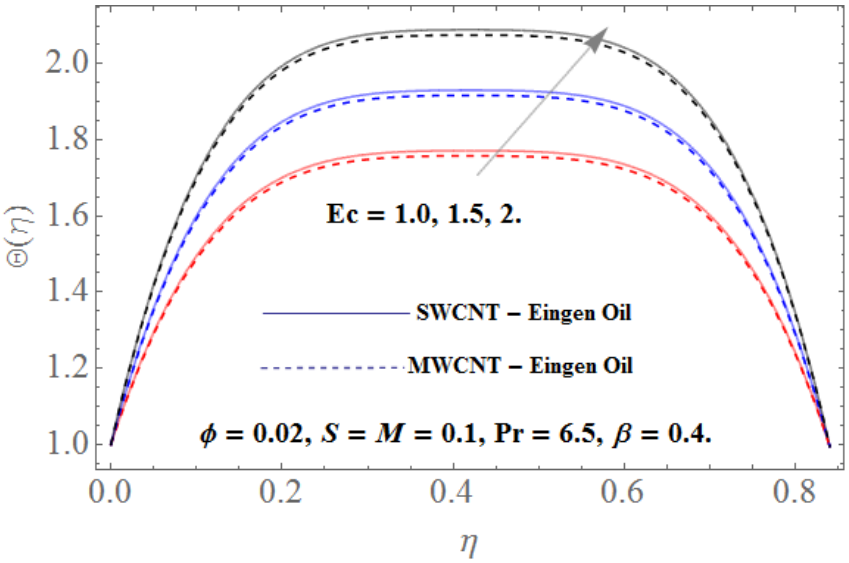

Figure. 11: The impact of the Eckert number Ec on the temperature field $\Theta(\eta)$.

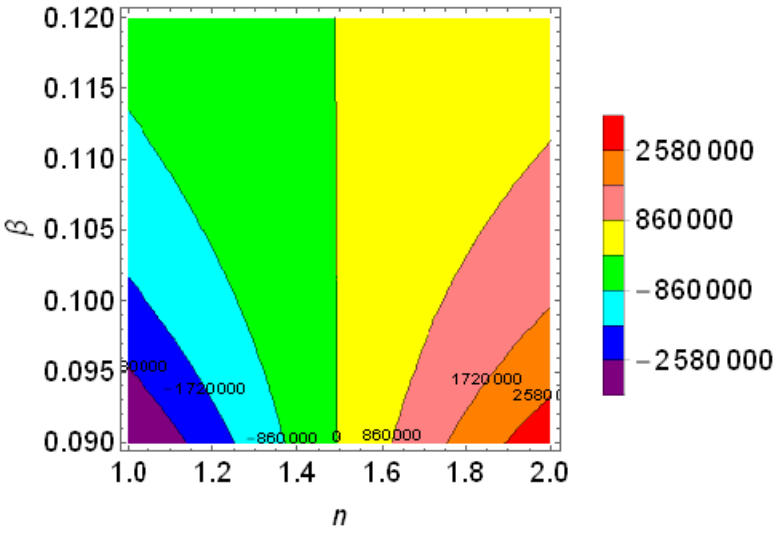

Figure 12: β versus n in the SWCNTs. When $x=3, \Pr=10.7, S=0.3, M=0.3, \phi=0.01$.

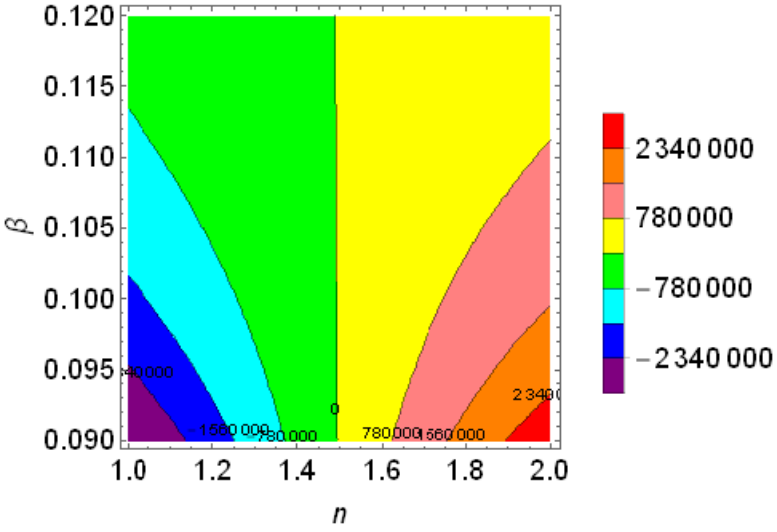

Figure. 13: β versus n in MWCNTs. when $x=3, \Pr=10.7, S=0.3, M=0.3, \phi=0.01$.

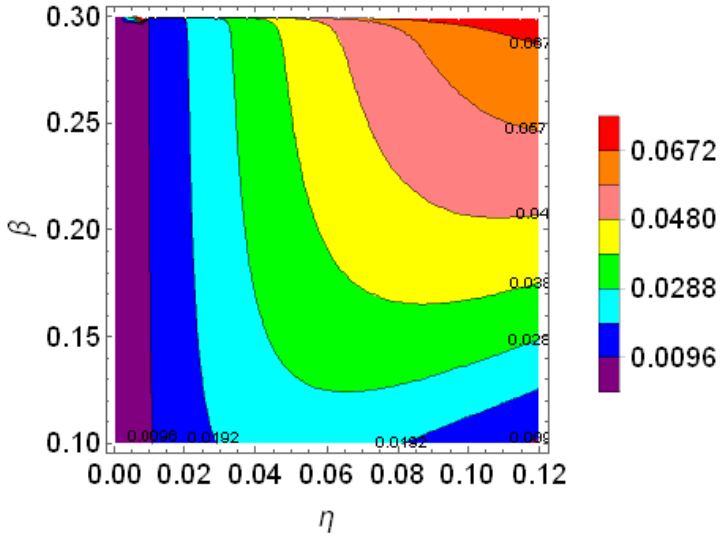

Figure 14: β versus x in SWCNTs. when $n=2, \Pr=10.7, S=0.3, M=0.3, \phi=0.01$.

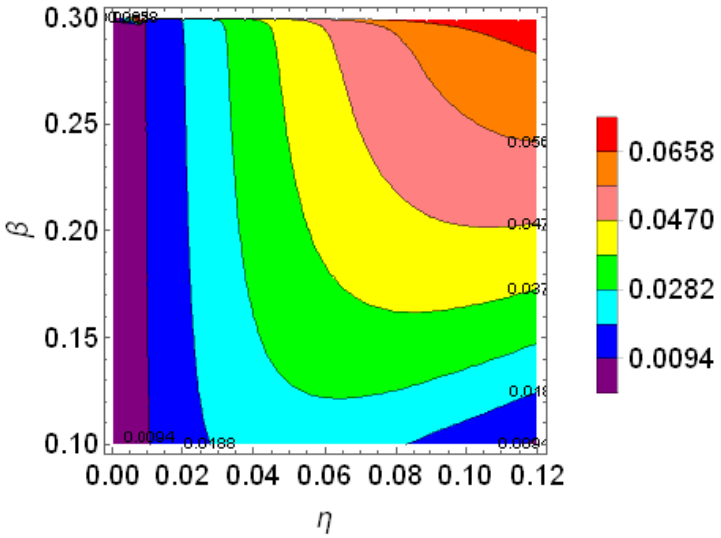

Figure. 15: β versus x in MWCNTs. when $n=2, \Pr=10.7, S=0.3, M=0.3, \phi=0.01.$

The larger amount of the unsteady parameter S declines the velocity profile and this effect is shown in Figure 3. Since the higher values of S enhancing the resistive force cause drop the radial velocity. The stretching fact is occurring by accelerating the value of nonlinearity n cause to decrease the flow motion as shown in Figure 4. In fact, the greater extent of n generating opposite force to drop the radial velocity, and this contrasting force is stronger in the MCNTs due to the closed compactness as compared to the SWCNTs. The impact of the magnetic parameter M for both sorts of CNTs (SWCNTs /MWCNTs) is presented in Figure 5. Keep in view greater values of the magnetic field M in engine oil based SWCNTs and MWCNTs reduce the radial velocity. The applied magnetic field B_0 creates induce current in the fluid to generate an opposing force (Lorentz force) which slow down the fluid velocity. The effect of β (thickness parameter) has been shown in Figure 6. The velocity field for both CNTs falls using the larger values of β. In fact, the thin nanofluid layer enhances the velocity, pitch and a smaller amount of energy is needed for the motion of fluid flow while the thick layer increases the resistance force to decline the radial velocity. Figure 7 exhibit the influence of nanoparticle φ on the streaming of CNTs nanofluid. We found that by raising the value of nanoparticle ϕ results enhance the radial velocity, pitch for both MWCNTs and SWCNTs. Actually, the thin liquid film, the greater extent of ϕ upsurge the energy, transport and a special type of force that is present among the molecules called cohesive force which helps the velocity progress. This effect is more ridiculous in the SWCNTs as compared to the MWCNTs. The difference in the two types of the CNTs is not clearly visible in the momentum boundary layer. In fact, the finite domain of the liquid film, the high nonlinearity of the problem and small volume fraction of the materials cause the difference between the two sorts of the CNTs.

The influence of ϕ versus thermal boundary layer has been exhibited in Figure 8. The thermal conductivity of the nanofluids depends on the particle volume fraction ϕ and the larger values of ϕ increases the temperature field. We noticed that decrease temperature profile and boost up the velocity, pitch for both MWCNTs and SWCNTs is gained in the range of $0 \le \phi \le 4\%$. The efficiency in the heat transfer enhancement of the SWCNTs is more visible using the thermal boundary layer as compared to the momentum boundary layer. The unsteadiness parameter S effect on the thermal

boundary layer has been depicted in Figure 9. The thickness of the boundary layer enhances with higher extent of S consequence the cooling effect rises to decline the temperature field. The larger values of the nonlinear stretching parameter n disturb the thin boundary layer and produce a cooling effect to reduce the CNTs nanofluid temperature as exhibited in Figure 10. Discussion of temperature distribution $\Theta(\eta)$ under the influence of Eckert number Ec has been depicted in Figure 11. Eckert number Ec consists of a dissipation term which creates viscous resistance result thermal conductivity enhance for its larger values and raise the temperature field. This effect is maximum in the SWCNTs due to the rapid improvement in the thermal conductivity.

The influence of the physical parameters in the contour form according to the obtained results for the range of parameters have been shown in Figs. [12-15] for the SWCNTs and MWCNTs respectively.

Table.1: Carrbon nanotubels and Engine oil thermo physical properties.

Physical Properties	Engine Oil	MWCNT	SWCNT
$\rho(Kgm^{-3})$	884	1600	2600
$Cp(J(kgK)^{-1})$	1910	796	425
$K(W(mK)^{-1})$	0.144	3000	6600

Table.2: Thermal conductivity of CNTs versus Volume fraction ϕ.

Volume fraction ϕ	0.0	0.01	0.02	0.03	0.04
k_{nf} for SWCNTs	0.145	0.174	0.204	0.235	0.266
k_{nf} for MWCNTs	0.145	0.172	0.2	0.228	0.257

Table 3: Individual averaged squared residual errors up to 20th order approximations, when β=1.1,Pr=6.7,M=S=Re=Gr=0.1, $\varphi = 0.01$.

m	ε_m^f *SWCNTs*	ε_m^f *MWCNTs*	ε_m^{Θ}*SWCNTs*	ε_m^{Θ}*MWCNTs*
6	5.0818×10^{-4}	3.1464×10^{-4}	2.0889×10^{-5}	1.8315×10^{-5}
10	1.5042×10^{-6}	0.9451×10^{-6}	3.2423×10^{-7}	2.843×10^{-7}
14	6.0317×10^{-8}	5.1421×10^{-8}	7.4416×10^{-9}	6.8371×10^{-9}
20	1.81121×10^{-9}	0.9213×10^{-9}	4.2869×10^{-11}	3.5920×10^{-11}

Table. 4: OHAM and Numerical (ND-Solve) comparison for $f(\eta)$. When $\beta = 1, M = 0.6, n = 1,\ \Pr = 6.7, \phi = 0.01, Ec = 1, S = 0.8.$

η	OHAM	ND-Solve
0.1	0.956789	1.000000
0.2	0.957369	0.992022
0.3	0.959098	0.985086
0.4	0.961942	0.979163
0.5	0.965847	0.974219
0.6	0.970737	0.970211

Table.5: Displays the effect of various parameters versus drage force coefficient $-f''(0)$.

n	S	β	$-f''(0)$ $\phi = 0.02$ SWCNTS	$-f''(0)$ $\phi = 0.04$ SWCNTS	$-f''(0)$ $\phi = 0.02$ MWCNTS	$-f''(0)$ $\phi = 0.04$ MWCNTS
2	0.1	0.3	0.03214	0.02921	0.02882	0.02601
3			0.04352	0.03911	0.03828	0.03722
4			0.05231	0.04371	0.04273	0.41673
	0.3		0.05529	0.04722	0.04629	0.04648
	0.5		0.05799	0.04968	0.04829	0.04722
		0.4	0.06429	0.05326	0.052428	0.05132
		0.5	0.07542	0.06420	0.06350	0.06219

Table.6: Displays the effect of various parameters versus $-\Theta'(0)$.

S	Ec	β	$-\Theta'(0)$ $\phi = 0.01$ SWCNTS	$-\Theta'(0)$ $\phi = 0.02$ SWCNTS	$-\Theta'(0)$ $\phi = 0.01$ MWCNTS	$-\Theta'(0)$ $\phi = 0.02$ MWCNTS
0.1	0.2	0.2	3.71635	6.13214	3.61754	4.72567
0.3			3.80213	6.16453	3.63243	4.81623
0.5			3.92217	6.20826	3.65346	4.95412
	0.3		3.60445	6.01308	3.1656	4.37524
	0.4		3.60255	6.0117	3.09636	4.1738
		0.3	4.42912	6.9238	4.01099	5.09259
		0.4	4.92398	7.21831	4.45952	6.18932

The thermophysical properties of the SWCNTs/MWCNTs and engine oil nanofluids is presented in Table 1. The thermal conductivity at different volume fraction for both types of CNTs are displayed in Table 2.The total residual error for the velocity and temperature fields using the OHAM technique has been displayed in Table.3. The obtained results are validated through numerical ND-Solve method and the outputs are demonstrated in Table 4. The influence of the physical constrants versus $\frac{d^2 f(0)}{d\eta^2}$ and $\frac{d\Theta(0)}{d\eta}$ have been shown in Tables 5,6. The higher values of n, S and β increasing $\frac{d^2 f(0)}{d\xi^2}$. In fact, the larger amount of nonlinearity, unsteadiness and thickness parameters, generate the opposing force which upsurges the skin friction. Increasing the thickness β and unsteadiness parameter S of the thin layer improving the opposite force to fluid flow and producing cooling effects to improve the Nusselt number demonstrated in Table 6. The greater values of Eckert number Ec, generally increasing the thermal conductivity and as a result, decline the Nusselt number. Temperature profile enhances due to thermal diffusivity and thermal diffusivity increase by increasing Ec.

1.4. Conclusion:

The flow of a liquid film comprising SWCNTs/MWCNTs-Engine oil based nanofluid over an unstable and flexible disc has been scrutinized in this article. The flexibility of the disc is considered nonlinear. The positive values change from linear $n=1$ to nonlinear $n=2,3,4....,$ which represent the nonlinearity of the flexible disc. The thickness of the liquid film also differs from thinning $\beta=0.01$ to thickening status $\beta=0.2,0.3,0.4....,$ for the vigorous outcomes. The dissipation term and magnetic effects also implemented to the flow Pattern. The difference in the two types of the CNTs is not clrealy visible in the momentum boundary layer while this change is more evident in the thermal boundary layer.

To accomplish the optimal values 20^{th} order of distortion for which the residual sum is minimized, we employed the provision of BVPh 2.0 package of OHAM technique. The summary of this article has been discussed in the following points.:

- The appropriate range of the physical parameters has been observed using the BVPh 2.0 package.
- The thermal efficiency of the MWCNTs is found less effective as compared to SWCNTs.
- The extending of the disc in nonlinear status decays the momentum and thermal boundary layers for both sorts of CNTs.
- The viscous dissipation enhancing the temperature distribution for its larger values and this consequence is more operative in the SWCNTs.
- The larger values of the nanoparticle volume fraction decline the viscosity of the nanofluid and increases the fluid motion and temperature profile.
- The confrontation force increasing with the greater values of the magnetic parameter to decline the nanofluid motion.
- The increasing thickness of the liquid film produces the confrontation force to decline the velocity field and this consequence is very agree for the both sorts of CNTs.

Numenclature:

ϕ solid particle volume fraction	n positive integer
ρ_{nf} density of the nanofluids	μ_{nf} dynamic viscosity of the nanofluids
k_f thermal conductivity of base fluid	k_{nf} thermal conductivity of the nanofluid
k_{CNT} thermal conductivities of the nanosolid particles	T temperature profile [K]
$(\rho C_p)_{nf}$ specific heat capacity of nanofluid	β dimensionless thickness of the liquid film
C_f skin friction	ρ_f density of the base fluid [kg/m^3]
T_b Ambient temperature [K]	t time
T_{ref} reference temperature [K]	S unstiness parameter
u velocity in the r-direction [m/s]	U_w surface velocity [m/s]
T_w Surface Temperature [K]	Pr Prandtl number
$(\rho c_p)_f$ Specific heat capacity of base fluid	w velocity in the z-direction [m/s]
η Similarity variable	μ_f Dynamic viscosity of base fluid
M magnetic parameter	r radial direction [m]
Re Reynolds number	z axis of the disk [m]

Competing Interests. The authors state that they have no competing interests.

Acknowledgement: This project was funded by the Deanship of Scientific Research (DSR), King Abdulaziz University, Jeddah, SA under grant no. (KEP-18-130-19). The authors, therefore, acknowledge with thanks DSR technical and financial support.

References

[1] Oberlin, A., Endo, M., Koyama, T., Filamentous growth of carbon through benzene decomposition, *J Cryst Growth,32* (1976), 3, pp. 335-49.

[2] Iijima, S., Helical microtubules of graphitic carbon, *Nature, 354* (199),11, pp. 56-64.

[3] Iijima, S., Ichihashi, T., Single-shell carbon nanotubes of 1-nm diameter, *Nature, 363* (1993),6,pp.603-605.

[4] Bethune, D. S., Kiang CH, Devries MS, Gorman G, Savoy R, Vazquez J, et al. Cobalt-catalysed growth of carbon nanotubes with single-atomic-layer walls. *Nature, 363* (1993), 6, pp. 605-607

[5] To C.W.S., Bending and shear moduli of single–walled carbon nanotubes, *Finite Elem Anal Des 42*, (2006), 5, pp.404–413.

[6] Terrones, M., Science and technology of the twenty-first century :synthesis, properties, and applications of carbon nanotubes, *An nu Rev Mater Res. 33*, (2003),12, pp.:419-501.

[7] De Volder, M.F.L et al., Carbon nanotubes: present and future commercial applications. *Science 339* ,(2013),2,pp. 535-543.

[8] Negin, C., Ali, S., Xie. Q., Application of nanotechnology for enhancing oil recovery, A review, *Petroleum, 2* (2016), 4, pp. 324-333.

[9] Murshed, S.M.S., Nieto de Castro. C.A., Superior thermal features of carbon nanotubes-based nano fluids -A review, *Renewable and Sustainable Energy Reviews, 37* (2014),9,pp. 155-167.

[10] Zaidi, Z., Mohyud-din, S .T., Mohsen, B.B., Convective heat transfer and MHD analysis of wall jet flow of nanofluids containing carbon nanotubes, *Eng. Comput., 34*(2017),3, pp. 1-9.

[11] Haq, R.U., Shahzad, F., Qasem, M., Al-Mdallal, MHD pulsatile flow of engine oil based carbon nanotubes between two concentric cylinders, *Results in Physics, 7* (2017), pp. 57-68.

[12] Xue, Q.,Model for thermal conductivity of carbon nanotube-based composites, *Phys B condens Matter, 368* (2005),11, pp.302–307.

[13] Garbadeen, I.D., Sharifpur, M., Slabber, J.M., Meyer, J.P., Experimental study on natural convection of MWCNT-water nanofluids in a square enclosure, *Int. Communications in Heat and Mass Transfer, 88* (2017), 11,pp. 1–8.

[14] Nasir, S. Islam, S., Gul, T., et al. Three‐dimensional rotating flow of MHD single wall carbon nanotubes over a stretching sheet in presence of thermal radiation. Applied Nanoscience, 8(2018),6, pp.1361-1378.

[15] Rehman, A.U., et al., Effects of single and multi-walled carbon nano tubes on water and engine oil based rotating fluids with internal heating, *Advanced Powder Technology,28* (2017),9, pp. 1991-2002.

[16] Ellahi, R., Hassan, M., Zeeshan, A., Study of Natural Convection MHD Nanofluid by Means of Single and Multiwalled Carbon Nanotubes Suspended in a Salt Water Solution, *IEEE Transactions on Nanotechnology, 14* (2015),July, pp. 1-10.

[17] Hayat, T., Nasir, T., Khan, M.I., Alsaedi, A., Non-Darcy flow of water-based single (SWCNTs) and multiple (MWCNTs) walls carbon nanotubes with multiple slip conditions due to rotating disk, *Results in Physics,* 9 (2018), June, pp. 390–399.

[18] Farooq,S., Hayat, T., Alsaedi, A., Asghar, S., Mixed convection peristalsis of corban nanotubes with thermal radiation and entropy generation, *J. of Molecular Liquids* , 250 (2018),January, pp. 451-467.

[19] Aman, S., Khan, I., Ismail, Z., Salleh, M.Z, Al-Mdallal, Q.A., Heat transfer enhancement in free convection fow of CNTs Maxwell nanofuids with four diferent types of molecular liquids. *Sci Rep*, 7 (2017), May,pp. 1–13

[20] Maxwell, J.C., Electricity and magnetism, 3rd ed. (clarendon, Oxford, 1904).

[21] Jaffery, D.J., Conduction through a random suspension of spheres, Proc Roy soc Lond. A., *Math. Phys. Sci., 335* (1973), Novemb, pp.335–36.

[22] Davis, R., The effective thermal conductivity of a composite material with spherical inclusions, *Int J Thermophys 7* (1986), pp. 609–620.

[23] Lu, S., Lin,H., Effective conductivity of composites containing aligned spherical inclusions of finite conductivity, *Journal of Applied Physics 79*(1998),June, pp. 6761–6769.

[24] Hamilton, R.I., Crosser, O.K., Thermal conductivity of heterogeneous two-component systems, *Ind. Eng. Chem. Fundam, 1* (1962) August, pp.182–91.

[25] Xue, Q., Model for thermal conductivity of carbon nanotube-based composites, *Phys B Condens Matter, 368* (2005), Nov, pp. 302–307.

[26] Shahzad, A., Ali,R., Khan, M., On the Exact Solution for Axisymmetric Flow and Heat Tra nsfer over a Nonlinear Radially Stretching Sheet, *CHIN. PHYS. LETT*, 29 (8) (2012) 084705,

[27] T. Hayat, S. Qayyum, M. Waqas, A. Alsaedi, Thermally radiative stagnation point flow of Maxwell nanofluid due to unsteady convectively heated stretched surface, *J. of Molecular Liquids*, 224 (2016) , Dec, pp. 801-810.

[28] T. Hayat, G. Bashir, M. Waqas, A. Alsaedi, MHD flow of Jeffrey liquid due to a nonlinear radially stretched sheet in presence of Newtonian heating, *Results in Physics*, 6 (2016) 817–823.

[29] M. Mustafa, J. A. Khan, T. Hayat, A. Alsaedi, Analytical and numerical solutions for axisymmetric flow of nanofluid due to non-linearly stretching sheet, *Int. J. of Non-Linear Mechanics*, 71(2015), May, pp.22-29.

[30] Wang, C.Y., Liquid film on an unsteady stretching surface, *Quart. Appl. Math. 48* (1990),4, pp.601–610.

[31] Gul, T., Scattering of a thin layer over a nonlinear radially extending surface with Magneto hydrodynamic and thermal dissipation. Surface Review and Letters, 26 (2018), 1, pp. 1-7.

[32] Ghani, F., *et al.:* Unsteady Magnetohydrodynamics Thin Film Flow of a third grade fluid over an oscillating inclined belt embedded in a porous medium Thermal Science, Year 2016, No. 5, pp. 875-887

[33] Gohar, T. Gul, T., et al., MWCNTs/SWCNTs Nanofluid Thin Film Flow over a Nonlinear Extending Disc: OHAM Solution, *J. of Thermal Science*, 28 (2019),1, pp.115-122.

[34] Qasim, M., Khan, Z.H., Lopez, R.J., Khan, W.A., Heat and mass transfer in nanofluid over an unsteady stretching sheet using Buongiorno's model, *Eur. Phys. J. Plus, 131* (2016), Jan,pp. 1–16.

[35] Wang, C.Y., Liquid film sprayed on a stretching cylinder, *Chem. Eng. Comm., 193* (2006),7, pp. 869–878.

[36] Khan, N.S.,Gul, T., et al., Magneto hydrodynamic Nanoliquid Thin Film Sprayed on a Stretching Cylinder with Heat Transfer, *Appl. Sci. 7* (2017), Mar, pp. 271-296.

[37] Alshomrani, A.S., Gul,T., A convective study of Al2O3-H2O and Cu-H2O nano-liquid films sprayed over a stretching cylinder with viscous dissipation, Eur. Phys. J. Plus, 132(2017), Nov, pp. 495-512.

[38] Liao, S.J.,The proposed homotopy analysis method for the solution of nonlinear problems, PhD Thesis, Shangai Jiao Tong Universit. (1992).

[39] Liao, S.J., Ed. Advances in the Homotopy Analysis Method, chapter7, World Scientific Press, (2013).

[40] Y. Zhao, Y. and Liao,S.J., Chapter 9: HAM-Based Mathematica Package BVPh 2.0 for Nonlinear Boundary Value Problems, Advance in the Homotopy Analysis Method, *world Scientific*, (2014), Jan, pp. 361-417.

[41] Farooq,U., Zhao,Y.L., Hayat,T., Alsaedi,A. Liao, S.J, Application of the HAM-based Mathematica package BVPh 2.0 on MHD Falkner–Skan flow of nano-fluid, Computers & Fluids, 111(16) (2015), April, Pp. 69-75

[42] Ellahi, R., M Hassan,M., Zeeshan,A., Shape effects of spherical and non-spherical nanoparticles in mixed convection flow over a vertical stretching permeable sheet, *Mech. of Adv. Mater. and Structures*, 24 (15) (2017), Feb, pp. 1231-1238.

[43] Ellahi,R., Zeeshan, A., Shehzad, N., Alamri,S.Z., Structural impact of Kerosene-Al2O3 nanoliquid on MHD Poiseuille flow with variable thermal conductivity: application of cooling process, J. of Molec. Liquids, 264 (15) (2018), August, pp. 607-615.

[44] Gul,T., Ferdous, K., The experimental study to examine the stable dispersion of the graphene nanoparticles and to look at the GO–H2O nanofluid flow between two rotating disks, *Applied Nanoscience*, 8 (7) (2018), pp. 1711–1727.

[45] Waqas, M., Hayat, T.,Alsaedi, A., A theoretical analysis of SWCNT–MWCNT and H2O nanoflids considering Darcy–Forchheimer relation, *Applied Nanoscience*, (2018), July, pp.19.